Tsunami inundation modeling for western Sumatra

***José C. Borrero*[*†‡], Kerry Sieh[§], Mohamed Chlieh[§], and Costas E. Synolakis*[*¶]**

**Department of Civil and Environmental Engineering, University of Southern California, Los Angeles, CA 90089-2531; [†]ASR Limited, Marine Consulting and Research, 1 Wainui Road, Raglan, New Zealand; [§]Tectonics Observatory 100-23, Division of Geological and Planetary Sciences, California Institute of Technology, Pasadena, CA 91125; and [¶]Laboratory of Natural Hazards and Coastal Engineering, Technical University of Crete, 73100 Chanea, Greece*

Author contributions: J.C.B., K.S., M.C., and C.E.S. designed research; J.C.B., K.S., and M.C. performed research; J.C.B., K.S., and M.C. analyzed data; and J.C.B., K.S., and C.E.S. wrote the paper.

The authors declare no conflict of interest.

This article is a PNAS direct submission.

[‡]To whom correspondence should be addressed. E-mail: jborrero@usc.edu.

This article contains supporting information online at www.pnas.org/cgi/content/full/0604069103/DC1.

Abstract

A long section of the Sunda megathrust south of the great tsunamigenic earthquakes of 2004 and 2005 is well advanced in its seismic cycle and a plausible candidate for rupture in the next few decades. Our computations of tsunami propagation and inundation yield model flow depths and inundations consistent with sparse historical accounts for the last great earthquakes there, in 1797 and 1833. Numerical model results from plausible future ruptures produce flow depths of several meters and inundation up to several kilometres inland near the most populous coastal cities. Our models of historical and future tsunamis

confirm a substantial exposure of coastal Sumatran communities to tsunami surges. Potential losses could be as great as those that occurred in Aceh in 2004.

Keywords: coastal engineering; earthquake; geophysics; natural disasters

Abbreviations: Mw, teleseismic moment magnitude; MOST, method of splitting tsunami.

The horrific impact of the 2004 tsunami on the Acehnese coast of Sumatra has evoked widespread concern about similarly devastating tsunamis on other populated coasts. One of the most plausible localities for a tsunami of disastrous proportions in the near future is the section of Sumatran coast southeast of the region affected by the 2004 event (Fig. 1). More than 1 million Indonesians live along this length of coast south of the Equator, about twice the pre-2004 population of the west coast of Aceh, ≈800,000 in Padang, 350,000 in Bengkulu, and tens of thousands more in smaller cities and villages along the coasts of the mainland and the Mentawai Islands.

Paleoseismic data suggest that great earthquakes recur about every 200 to 240 years along the adjacent section of the Sunda megathrust (4). The most recent of these occurred as a closely spaced couplet in 1797 and 1833 (5). Simple calculations of the average recurrence interval, made by dividing the average slip in 1797 (≈6 m) and 1833 (10–14 m) by the convergence rate of 45 mm/year, yield intervals ranging from 130 to 300 years. Thus, the average interval between great earthquakes (or couplets, as in 1797 and 1833) is nearly equal to the current dormant period. Moreover, calculations show that the ruptures of 2004 and 2005 have brought this section even closer to failure (6, 7). The possible imminence of a great earthquake and tsunami along this section of the Sumatran coast motivate this exploration of the characteristics of past and future tsunamis there.

Megathrust Models

One necessary input for any plausible tsunami model is the pattern of seafloor deformation. Fortunately, the extent of the deformations that produced the 1797 and 1833 tsunamis are relatively well known from the patterns of uplifted coral on the Mentawai Islands (5, 8). These data show that the 1797 rupture extended from 0.5° to 3.2° S (a distance of ≈300 km), average slip on the megathrust was ≈6 m, and the magnitude of the earthquake was between 8.4 and 8.6 (5). Uniform-slip rupture with these dimensions yields the patterns of uplift shown in Fig. 2*A*. The uplifted corals also imply that the 1833 rupture extended from ≈2.1°S to at least 5°S (a distance of at least 320 km), with slip possibly reaching 18 m, and a magnitude between 8.6 and 8.9 (Fig. 2*B*).

Having inferred these basic input parameters for the historical tsunamis of 1797 and 1833, we begin our modeling with an attempt to characterize these two events and compare model results against sparse historical reports of damage to coastal settlements. We then investigate tsunamis produced by four plausible future ruptures of the Mentawai section of the megathrust. Each of these scenarios spans the entire 750-km length of the currently locked patch south of the Equator, as deduced by Global Positioning System measurements, observations of subsiding corals on the islands and patterns of background seismicity (Fig. 1) (5, 9). Thus, they represent what we consider to be the longest plausible future ruptures. All of these scenarios are larger than the 1797 and 1833 ruptures, producing earthquakes ranging in size from teleseismic moment magnitude (Mw) 9.0 to 9.3 (Table 1).

In scenarios 1 and 2 (Fig. 2 C and D), the slip on the megathrust is uniformly 10 m, just under the maximum values that occurred during the 2005 Nias-Simeulue earthquake (10). In scenarios 3 and 4 (Fig. 2 E and F), the slip is uniformly 20 m, close to the maximum values that occurred during the 2004 Aceh-Andaman earthquake (11). In two of these four cases, scenarios 1 and 3, slip extends to the trench, as it may have along parts of the 2004 Aceh-Andaman rupture. In the other two cases, scenarios 2 and 4, the rupture does not extend to the trench, as was clearly the case for the 2005 Nias-Simeulue

event. Thus, our Mw-9.3 scenario 3, in which slip is 20 m and extends to the trench, should be viewed as an extreme rupture scenario. These source parameters would be roughly equivalent to those of the great Alaskan earthquake of 1964 (12).

Tsunami Modeling

To simulate the tsunami generated by these sources, we used the model MOST (method of splitting tsunami) (13–15), one of only two fully validated hydrodynamic models for operational tsunami propagation and inundation. MOST uses the final dislocation field from the seismic deformation model to initialize hydrodynamic computations.

MOST takes into account the onland crustal deformation from the earthquake and computes the wave evolution and run-up onto dry land over the newly deformed bathymetry and topography. Postseismic field investigations after the 2005 Nias-Simeulue earthquake demonstrated that the details of local coseismic deformation are of first-order importance to local tsunami inundation (J.C.B., unpublished data). In that case, local uplift during the earthquake diminished the severity of tsunami inundation on the offshore islands, whereas coseismic subsidence along the Sumatran mainland allowed tsunami waves to penetrate further inland, causing more damage and flooding than otherwise. In the scenarios computed here, the same phenomena occur; the Mentawai Islands rise and the mainland coast subsides during the seismic rupture.

To perform accurate modeling of tsunami inundation and run up, a detailed model of nearshore bathymetry and coastal topography is necessary. Because data at the resolution necessary for meaningful inundation mapping were not readily available, we digitized the appropriate nautical charts and combined these with publicly available deep water bathymetry and near shore topography.|| The data were inspected, compared with aerial photography (http://earth.google.com), and manually adjusted as needed to reflect more accurately the coastal topography in the areas of interest.

MOST uses a system of three nested rectangular computational grids in geophysical coordinates, thus permitting efficient numerical solution over a wide area. Regions far from the area of interest were modeled with 1,200- and 600-m coarser outer grids, whereas the specific study areas of Padang and Bengkulu were modeled at 200-m resolution. We performed full-inundation computations at 200-m resolution to avoid the well known underestimation issues that plague threshold models that stop the calculation at some offshore depth (16). Although 200-m grids are on the borderline for being too coarse, limitations in the available source data for creating the computational grids prevented us from using higher-resolution grids. Future inundation studies for creating operational inundation maps should consider using a finer-grid spacing for greater detail. For reference, most existing inundation maps in California were produced at a resolution ranging from 75 to 250 m (17).

Results and Discussion

Fig. 3 shows inundated areas and computed flow depths over land for a subset of the modeled scenarios: 1797 at Padang, 1833 at Bengkulu, and scenarios 1 and 3 at both cities. Along the 8-km length of coast near Padang shown in Fig. 3, we calculate shoreline flow depths for 1797 ranging from ≈1.5 to 4m(Fig. 3*A*). Inundation distances are generally ≈600 m, except along the river, where the town was clustered in 1797, where the inundation distance is about a kilometer. This result is consistent with reports of a 200-ton English vessel being carried into the town, about a kilometre upstream from its mooring near the river mouth and with small vessels being carried even farther inland (5). Flow depths at the town might have exceeded 5 m, judging from these accounts. Our results may underestimate the actual tsunami parameters by about a factor of two at the old settlement. Changes in onshore coastal topography that may have occurred in the past 200 years do affect inundation parameters to first order (18). However, land-level changes are known to introduce uncertainty of this order when hindcasting tsunamis from historic events and projections are judged by the preponderance of evidence (19–21). We also suspect that underestimation may also result from an underestimate of slip under and

southwest of Siberut island, the large island between Padang and the trench, because slip on that section of the 1797 rupture was based on coral uplift data at just one point on the northeast side of the island (5).

Along the 11-km section of the Bengkulu coast displayed in Fig. 3, we calculate shoreline flow depths ranging from 1 to 4 m for the 1833 tsunami. Inundation distances along the coast range from 0.4 to 1.5 km. The greatest inundation distance occurs in a low-lying swamp and river floodplain. Flow depths of nearly 4 m and inundation distances of half a kilometer at the old wharf are consistent with reports that the 1833 tsunami destroyed the wharf and customs house (5).

Our model results for the 1797 and 1833 events show contrasting effects at Bengkulu and Padang that ref lect what is known from available historical information. For the 1797 event, the modeled offshore wave heights at Padang (≈2 m) are much larger than at Bengkulu (≈0.6 m), whereas for the 1833 event the opposite is true (≈2 m at Padang versus ≈3 m at Bengkulu). These differences are expected intuitively because the source of the 1797 tsunami was closer to Padang, whereas the source of the 1833 event was closer to Bengkulu (Fig. 2). Historical accounts (5) suggest that the 1797 tsunami was, indeed, more severe in Padang than in Bengkulu and that the opposite was true for the 1833 event. Moreover, historical accounts of the 1797 tsunami describe three or four successive ebbs and surges of the sea at Padang, also consistent with our synthetic mareogram, which depicts three distinct crests in the first 90 min (Fig. 3). Mareogram projections do not depend on onshore topography.

Scenarios 1 and 3 result from sources with 10 and 20 m of slip, respectively, in each case extending up dip to the trench (Fig. 2 *C* and *E*). Surprisingly, the companion scenarios (2 and 4), with the same slip values, but not extending to the trench, yield results that are similar. Because of the larger slip amounts, the flow depths and inundation distances in each of these cases are greater than in 1797 and 1833 (Fig. 3). The general form of the mareograms is similar to the 1797 and 1833 mareograms,

however; three short-duration inundation crests between 0.6 and 1.2 h at Padang and broad surge crests at ≈0.8 h and 2.5 h at Bengkulu.

The maximum crest heights just offshore of Padang and Bengkulu are ≈3 and 6 m, respectively, for scenario 1 (10-m slip on the megathrust). Inundation distances are 0.6–1 km at Padang and 0.4–3 km near Bengkulu. Generally, inundation and flow depths are ≈50% greater in scenario 1 than during the model 1797 and 1833 events. Maximum crest heights offshore Padang and Bengkulu are 5 and 8 m, respectively, for scenario 3 (20-m slip on the megathrust), with inundation distances ranging from 1 to 2 kmat Padang and 0.6 to 6 km near Bengkulu.

Modeled tsunami impacts associated with scenario 3 are qualitatively similar to those observed after the 2004 Aceh tsunami, with shoreline flow depths of 10 m or greater and locally extensive inland inundation (22). The greatest modelled inundation distances are in locations analogous to the coastal Acehnese wetlands and river flood plains that were hard hit in 2004 (23).

In all four future scenarios, coastal areas in and around Bengkulu generally suffer greater inundation than the region of Padang. Padang probably owes this relatively good fortune to the presence of the Mentawai Islands offshore. They likely shield the adjacent mainland coast from the direct impact of the region of maximum seafloor uplift, southwest of the islands (Fig. 2). As there are no large islands offshore of Bengkulu, that reach of the mainland coast is exposed to the direct impact of the region of maximum uplift. In this respect, the coast near Bengkulu resembles the west coast of Aceh, as devastated in 2004 by the impact of waves that were not affected by the presence of offshore islands. By contrast, the Padang coast is analogous to the coast of North Sumatra, which suffered far less devastating tsunami inundation in 2005, ascribable at least in part to the presence of the large island of Nias between itself and the region of maximum seafloor uplift (10, 24, 25). Supporting information (SI) Movies 1–10 are related to tsunami wave propagation and inundation for a subset of the cases described here. Each movie depicts the tsunami propagation for the first 3 h after initiation of the

megathrust rupture. SI Movies 1–4 depict the entire Sumatran region for the tsunamis of 1797, 1833, and scenarios 2 and 4, and SI Movies 6–10 focus on the near field effects in Padang and Bengkulu for 1797, 1833, and scenarios 1 and 3.

The consistency of our models of the 1797 and 1833 tsunami with sparse historical accounts lends credibility to our modeling approach. The large inundation distances and flow depths in the four scenarios suggest that coastal Sumatran communities south of the Equator have a serious exposure to tsunamis. Clearly, the dangers posed by 20 m of slip on the megathrust, similar to that which occurred offshore Aceh in 2004, are greater than those posed by just 10 m of slip, as occurred offshore of North Sumatra in 2005. Moreover, coasts directly exposed to the region of maximum seafloor uplift are likely to experience greater flow depths and inundation distances than those offered some protection by intervening islands. Nonetheless, hundreds of thousands of the residents of coastal West Sumatra and Bengkulu provinces are at risk from tsunami surges that will result from the next great ruptures of the Sunda megathrust beneath the Mentawai islands.

We hope that our simulations of a range of plausible scenarios will motivate better assessments of site-specific tsunami hazard along the Sumatran coast and help accelerate hazard mitigation activities in the region. When the next great Mentawai earthquake strikes, the communities of West Sumatra and Bengkulu provinces must be more adequately prepared if they are to escape the fate of the Acehnese coast in 2004.

[‖]Nautical charts of 1:250,000 scale from the Indonesian hydrographic service were scanned and geo-referenced to latitude/longitude coordinates by using the appropriate datum (UTM48-S, Batavia) and spheroid (Bessel 1841), as specified on the charts. All contours, soundings, and land elevations on the charts were then digitized by hand. These data were then combined with the SRTM30_PLUS data set (http://topex.ucsd.edu) to generate a combined map containing near and offshore bathymetry and coastal topography. The combined data set was then interpolated to a 200-m grid in latitude/longitude coordinates in the WGS84 projection.

References

1. Gudmundsson O, Sambridge M (1998) *J Geophys Res* 103:7121–7136.
2. Natawidjaja D, Sieh K, Ward S, Edwards R, Galetzka J, Suwargadi B (2004) *J Geophys Res*, 10.1029/2003JB002398.
3. Rivera L, Sieh K, Helmberger D, Natawidjaja D (2002) *B Seismol Soc Am* 92:1721–1736.
4. Sieh K (2006) *Philos Trans R Soc London A* 364:1947–1963.
5. Natawidjaja D, Sieh D, Chlieh M, Galetzka J, Suwargadi B, Cheng H, Edwards R, Avouac J-P, Ward S (2006) *J Geophys Res*, 10.1029/2005JB004025.
6. Nalbant S, Steacy S, Sieh K, Natawidjaja D, McCloskey J (2005) *Nature* 435:756–757.
7. Pollitz F, Banerjee P, Bürgmann R, Hashimoto M, Choosakul N (2006) *Geophys Res Lett*, 10.1029/2005GL024558.
8. Zachariasen J, Sieh K, Taylor F, Edwards R, Hantoro W (1999) *J Geophys Res* 104:895–920.
9. Abercrombie R, Antolik M, Ekstrom G, (2003) *J Geophys Res*, 10.1029/2001JB000674.
10. Briggs R, Sieh K, Meltzner A, Natawidjaja D, Galetzka J, Suwargadi B, Hsu Y-J, Simons M, Hananto N, Suprihanto I, *et al.* (2006) *Science* 311:1897–1901.
11. Subarya C, Chlieh M, Prawirodirdjo L, Avouac J-P, McCaffrey R, Bock Y, Sieh K, Meltzner A-J, Natawidjaja D (2006) *Nature* 440:46–51.
12. Plafker G (1969) *Tectonics of the March 27, 1964, Alaska Earthquake* (U.S.Geological Survey, Reston, VA), Paper 543-I.
13. Titov V, Synolakis C (1997) *J Waterw Port C Div* 124:157–171.
14. Titov V, Gonzalez F (1997) *Implementation and Testing of the Method of Splitting Tsuna*mi *(MOST)* (National Oceanic and Atmospheric Administration, Washington, DC), Technical Memorandum ERL PMEL-112.
15. Titov V, Rabinovich A, Mofjeld H, Thomson R, Gonzalez F (2005) *Science* 309: 2045–2048.
16. Synolakis C, Bernard E (2006) *Philos Trans R Soc London A* 364:2231–2265.
17. Borrero J, Dolan J, Synolakis C (2001) *Geophys Res Lett* 28:643–647.

18. Kanoglu U, Synolakis C (1998) *J Fluid Mech* 374:1–28.
19. Synolakis C (1995) *Science* 270:15–16.
20. Satake K, Shimazaki K, Tsuji Y, Ueda K (1996) *Nature* 379:246–249.
21. Satake K, Wang K, Atwater B (2003) *J Geophys Res*, 10.1029/2003B002521.
22. Borrero J (2005) *Science* 308:1596.
23. Geist E, Titov V, Synolakis C (2005) *Sci Am* 294:56–65.
24. Kerr R (2005) *Science* 308:341.
25. Geist E, Bilek S, Arcas D, Titov V (2006) *Earth Planets Space* 58:185–193.

List of Tables

List of Figures

seriously impacted by future tsunamis. The effects at Bengkulu, unprotected by offshore islands, will likely be more severe than at Padang.

Scenario (magnitude)	Segment	Upper-middle segment		Half-length, km	Depth, km	Slip, m
		Longitude, °	Latitude, °			
1797 (M_w = 8.7)	1	98.2	−1.8	110	5–40	6
	2	99.0	−2.8	35	5–34	8
	3	99.3	−3.3	33	5–38	6
	4	99.6	−3.6	8	5–45	4
1833 (M_w = 8.9)	1	99.0	−2.9	15	5–50	9
	2	99.3	−3.3	35	5–50	11
	3	100.0	−4.2	90	5–37	18
S1 (M_w = 9.0)	1	98.3	−2.0	130	5–40	10
	2	100.0	−4.2	180	5–50	10
	3	101.4	−6.0	70	5–25	10
S2 (M_w = 8.9)	1	98.3	−2.0	130	15–40	10
	2	100.0	−4.2	180	15–50	10
	3	101.4	−6.0	70	15–50	10
S3 (M_w = 9.3)	1	98.3	−2.0	130	5–40	20
	2	100.0	−4.2	180	5–50	20
	3	101.4	−6.0	70	5–50	20
S4 (M_w = 9.1)	1	98.3	−2.0	130	15–40	20
	2	100.0	−4.2	180	15–50	20
	3	101.4	−6.0	70	15–50	20

Table 1

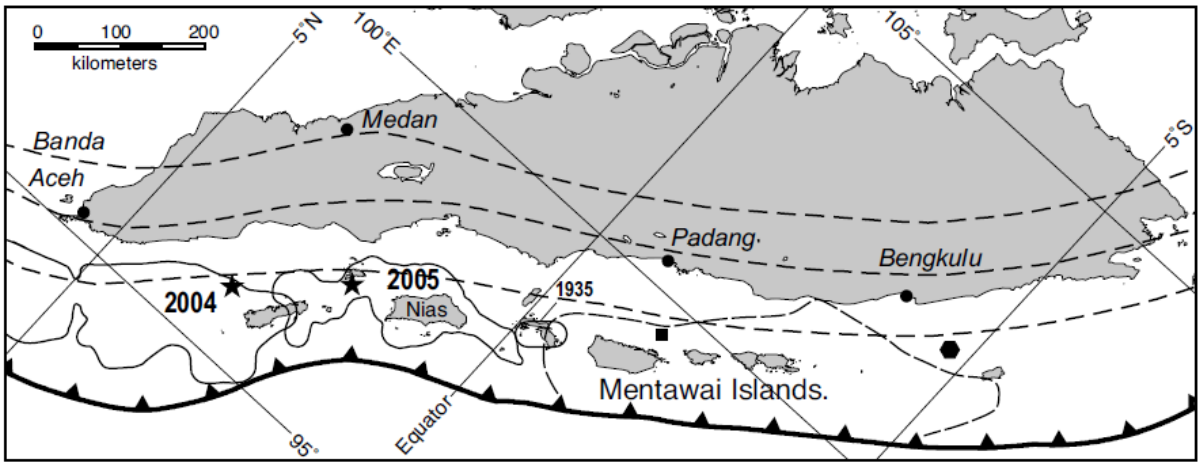
0 100 200
kilometers
5°N
100°E
105°
5°S
95°
Equator
Banda
Aceh
Medan
Padang
Bengkulu
2004
2005
Nias
1935
Mentawai Islands.

Fig. 1

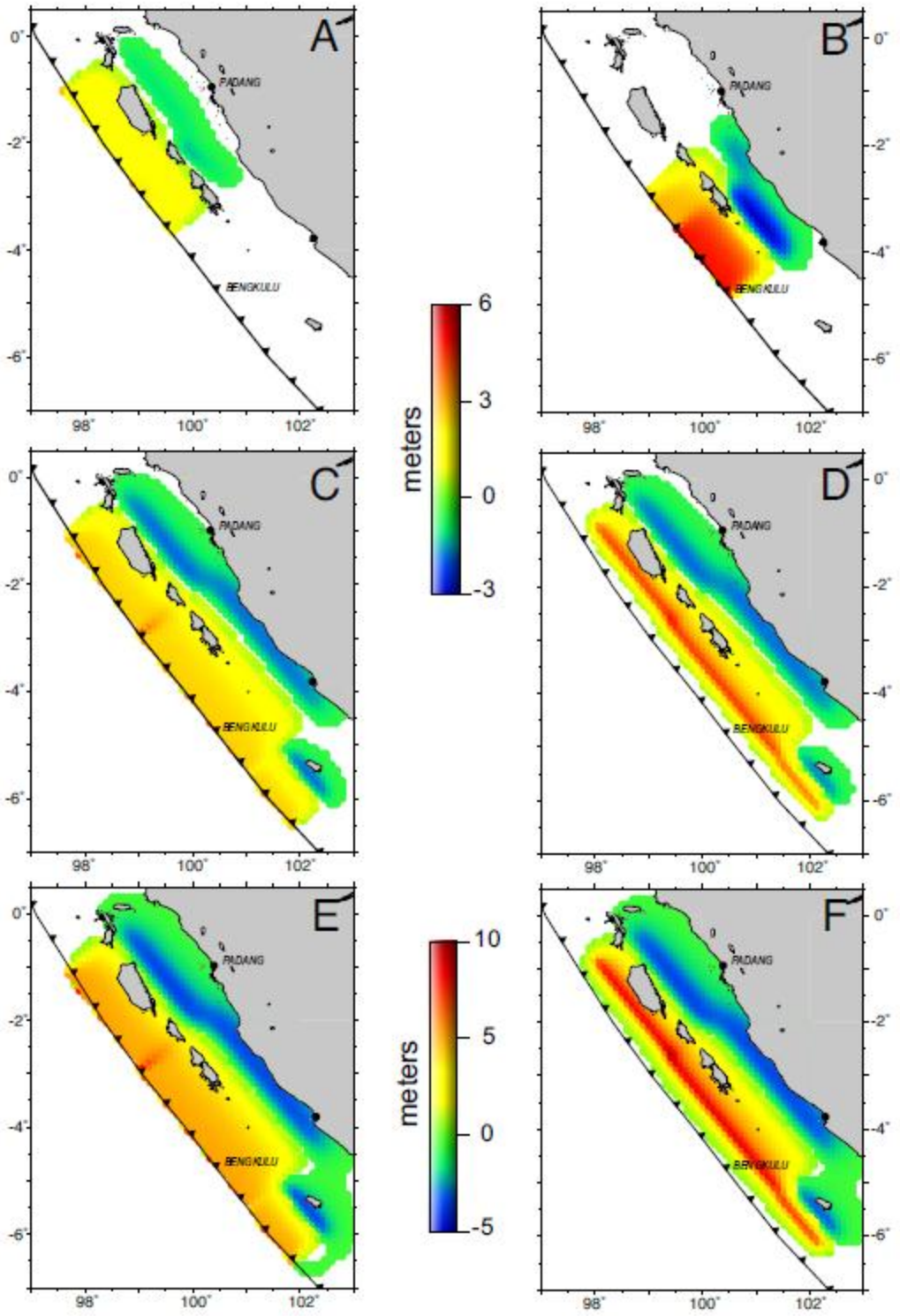

Fig. 2

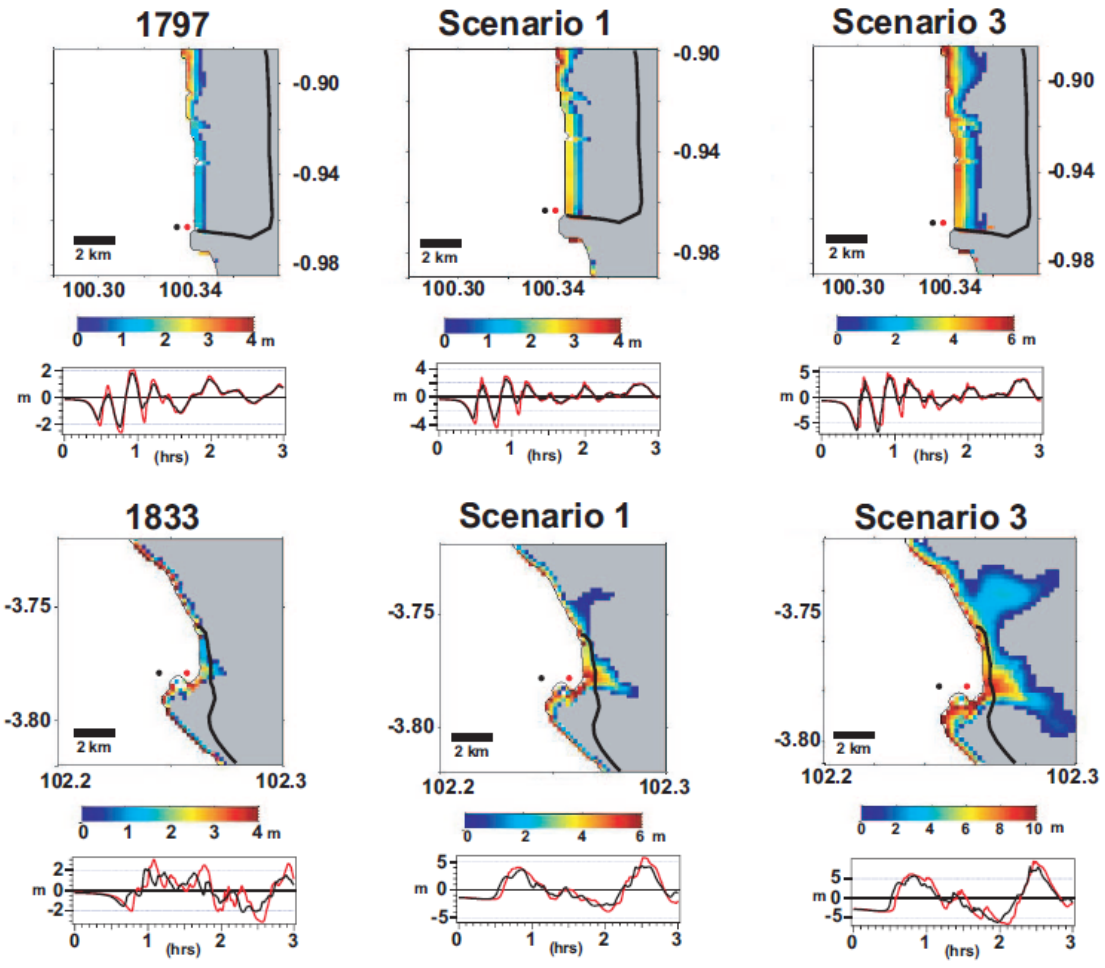
1797
Scenario 1
Scenario 3
-0.90
-0.94
-0.98
2 km
100.30
100.34
0 1 2 3 4 m
0 2 4 6 m
m
(hrs)
1833
-3.75
-3.80
102.2
102.3
0 2 4 6 8 10 m

Fig. 3